3-1-2001

Study of surface chemical changes and erosion rates for CV-1144-O silicone under electron cyclotron resonance oxygen plasma exposure

Li Yan
University of Nebraska - Lincoln

Xiang Gao
University of Nebraska - Lincoln

Corey Bungay
University of Nebraska - Lincoln

John A. Woollam
University of Nebraska - Lincoln

Study of surface chemical changes and erosion rates for CV-1144-O silicone under electron cyclotron resonance oxygen plasma exposure

Li Yan,[a] Xiang Gao, Corey Bungay, and John A. Woollam
Center for Microelectronic and Optical Materials Research, Department of Electrical Engineering,
University of Nebraska–Lincoln, Lincoln, Nebraska 68588-0511

CV-1144-O silicone thin films were irradiated in an electron cyclotron resonance oxygen plasma, which is a simulation of the low earth orbital environment. A crude equivalence between this plasma system and the low earth orbital environment was determined by measuring Kapton weight loss in the plasma and comparing to Kapton weight loss in space experiments. Changes in optical properties and erosion rates under ultraviolet light and atomic oxygen radiation were studied using *in situ* spectroscopic ellipsometry (SE). The erosion rate at the beginning of the plasma exposure was significantly faster than that at later stages. Approximately one third of the total silicone thickness was etched away within 1 h, which according to the equivalence experiment, corresponds to about two months in low earth orbit. The refractive index of silicone in the visible range increased during the exposure, indicating that the film was being densified. Optical constants (both before and after plasma exposure) were determined by *ex situ* spectroscopic ellipsometry in the ultraviolet–visible–near-infrared (0.7–8.5 eV) and IR (200–7000 cm^{-1}) ranges. Also, SE was used to map thickness and uniformity before and after radiation. Regression fits using Lorentzian and Gaussian oscillators as parametric models for the optical constants were excellent, and the major absorption peaks in the IR region were identified. The before- and after-radiation spectra showed significant decreases in CH$_3$-associated peaks and increases in SiO$_x$-associated peaks. © *2001 American Vacuum Society.* [DOI: 10.1116/1.1340652]

I. INTRODUCTION

Material degradation arising from atomic oxygen (AO) attack is an important long-term issue for spacecraft orbiting in low earth orbit (LEO). Many spacecraft, such as the U.S. Space Shuttle, the Russian Mir Space Station, and the Hubble Telescope, circle the earth in low earth orbit, where the residual atmosphere is composed predominantly of oxygen (80%) and nitrogen molecules (20%).[1,2] In low earth orbit, atomic oxygen is generated by photodissociation of diatomic oxygen under ultraviolet (UV) radiation from the sun, and exists where the mean-free path of atomic oxygen is large enough that recombination has low probability.[2–5] The atomic oxygen density in LEO is not particularly high, depending strongly on solar activity and position; however, because of the high orbital velocity (approximately 8 km/s at Shuttle altitude), the flux is quite high, of the order of 10^{15} atoms/cm^2 s.[6] The atomic oxygen in the LEO environment has caused deleterious erosion and oxidation problems for spacecraft materials.[3–5,7,8] Furthermore, contamination due to the eroded products that come from one region of a spacecraft and land in another region has become another significant problem. For example, silicone exposed to AO on one part of the spacecraft can redeposit material on solar cell surfaces, degrading power generation.[9]

It is possible to apply very thin coatings onto the exposed surfaces of spacecraft in order to protect them from harmful AO damage.[10] The application and durability of different coating materials have been studied for years.[3–5,7,11–14] Coatings of inorganic oxides such as aluminum oxide, silicon oxide, chromium oxide, as well as decaborane-containing polymers, have been shown to protect organic materials against oxygen plasma and/or AO erosion.[15] Lately, attention has been focused on the use of polymeric materials as protective coatings due to the ease and flexibility of their application.[2] A class of noncarbon-based materials with erosion rates one to two orders of magnitude lower than organic polymers in LEO are the silioxane polymers, which, when exposed to AO radiation, convert to a protective silica-like coatings.[10,16] Silicones, which are inorganic polymers,[17] have been used extensively as a protective coating material in space. It is found that silicone can chemically change into an ultraviolet resistant material upon AO and UV irradiation, which will serve as a barrier protecting underlying oxidizable materials. Upon reaction with atomic oxygen the silicone coatings ($d \approx 1$ g/cm^3) lose their organic components and undergo a density increase to somewhere near that of amorphous SiO$_2$ ($d \approx 2.4$ g/cm^3).[2] Also, ground-based tests

FIG. 1. CV-1144-O chemical structure.

---

[a]Electronic mail: yanli75@yahoo.com

TABLE I. CV-1144-O silicone samples. Note: (1) The volume ratio of silicon to Naptha (*V/V*) was 1:100 for samples 2C–3E, and it was 1:15, 1:5, and 1:10 for sample Nos. 1, 6, and 7, separately. (2) Spin time: 50 s.

Sample	2C	2O	2T	3A	3B	3C	3D	3E	No. 1	No. 6	No. 7
Thickness, (nm)	41.9	45.1	45.9	39.1	35.8	39.3	33.5	30.8	244.9	1076	369.4
Mapping (bef. AO)	×[a]	×	×								
UV-VIS (bef. AO)	×	×	×	×	×	×	×	×	×	×	×
Deep UV (bef. AO)				×	×	×		×			
IR (bef. AO)	×	×	×		×			×	×	×	×
AO exposure	×	×	×	×	×	×		×		×	
Exposure condition	100 W 1.0 sccm 30 mins	60 W 2.0 sccm 1.0 h	60 W 1.0 sccm 1.0 h	100 W 2.0 sccm 2.0 h	60 W 1.0 sccm 2.0 h	100 W 2.0 sccm 2.0 h	100 W 1.0 sccm 2.0 h	60 W 2.0 sccm 2.0 h		100 W 2.0 sccm 5.0 h	
UV–VIS (aft. AO)	×	×	×	×				×			
In situ SE					×	×	×			×	
IR (aft. AO)	×	×	×		×			×			
Deep UV (aft. AO)				×	×	×		×			

[a]Measurement was taken.

have shown that silicones exposed to atomic oxygen and vacuum UV radiation release polymeric fragments which deposit on neighboring surfaces, resulting in shortening of their operating time. This background information leads to questions related to silicone contamination problems, including physical and chemical changes to the surfaces exposed to AO radiation, the speed and origin of the surface chemical changes, and the nature of the eroded product.

Knowledge of the durability of materials operating in LEO is crucial to numerous space missions.[11,12,18] The effect of AO on spacecraft materials degradation has been studied on space-exposed materials [STS missions and NASA Long Duration Exposure Facility (LDEF)] and in simulation facilities.[19,20] Until recently, very limited flight data have been obtained from space due to costs associated with in-space experiments. Meanwhile, a large amount of work has been devoted to the development of AO facilities to simulate the LEO environment.[21] Exact simulation of the AO environment of LEO is difficult to achieve in an earth-based laboratory. Three general techniques have been used to simulate this environment: 60 Hz or radio-frequency (rf) oxygen plasmas, microwave oxygen plasmas, and atomic oxygen beams. Each technique has its own specific characteristics that approximate the LEO environment to some extent. Ground-based simulators make accelerated testing possible, assuming

that for constant fluence ($F = \Phi \times$ time, where Φ is flux) test, material reaction efficiency (R_e, also know as the erosion yield) will be the same.[21]

CV-1144-O silicone is a dimethyl diphenyl silicone co-polymer developed by NuSil Technology. Its chemical structure is shown in Fig. 1. In our previous work, the LEO environment was simulated with a rf oxygen plasma, and conversion of CV-1144-O silicone to silicon oxide was seen using infrared spectroscopic ellipsometry (SE) analysis.[22] By contrast, the atomic oxygen environment was simulated using an electron cyclotron resonance (ECR) oxygen plasma in this study, and the CV-1144-O erosion process was monitored by *in situ* spectroscopy ellipsometry. Changes in refractive index and erosion rates with time were quantitatively determined using *in situ* SE data analysis. In addition, optical and surface chemical changes of CV-1144-O silicone due to the AO radiation were also studied by vacuum ultraviolet (VUV) SE, UV–visible–near-infrared (UV–VIS–NIR) SE, and infrared (IR) SE. The optical constants before and after AO radiation were determined in the VUV–UV–VIS–NIR range as well as the IR range, using Lorentzian and Gaussian oscillators. Furthermore, the center energies of these oscillators were identified for both before- and after-AO optical constants in the IR range.
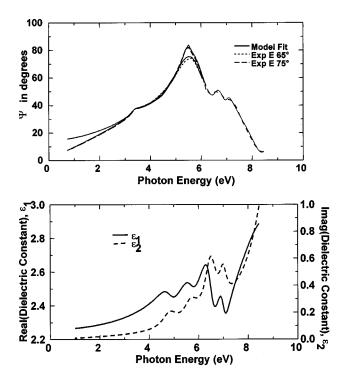
FIG. 2. VUV–UV–VIS–NIR raw data obtained from sample 3B, combined with a Lorentz model fit.

II. EXPERIMENTAL RESULTS AND ANALYSIS

A. Experiment

1. Sample preparation

Thin films of CV-1144-O silicone were spin coated onto different substrates, including polished silicon wafers (highly doped, as well as undoped), and optically thick sputter deposited films of Au, Pt, and Ir. Prior to spin coating, both UV–VIS–NIR SE data and IR SE data were taken on the substrates in order to provide accurate substrate optical constants for data analysis of the CV-1144-O films. A wide range of film thicknesses (starting from 30 nm to about 1000 nm) were obtained by adjusting the ratio of CV-1144-O to Naptha (solvent), the revolutions per minute (RPM), and the number of drops applied in a spin-coating process. A labeling of the samples used in our study, together with a listing of the experiments performed, are shown in Table I.

2. Atomic oxygen (plasma) chamber

An ECR oxygen plasma chamber was used to simulate the LEO environment. The nominal power of the ECR was

TABLE II. Oscillator constants in VUV–UV–VIS–NIR region (before AO exposure).

Oscillators	E_n (eV)	A_m (eV^2)	B_r (eV)
1	4.258 8	0.849 9	0.688 37
2	5.831 4	0.175 05	0.314 96
3	6.426 9	1.096 2	0.440 21
4	6.986 1	1.843 5	0.828 61
5	9.261 3	30.211	1.585 2

TABLE III. Oscillator constants in VUV–UV–VIS–NIR region (after AO exposure).

Oscillators	E_n (eV)	A_m (eV^2)	B_r (eV)
1	4.44	1.401 3	1.460 2
2	6.4383	0.271 03	0.592 55
3	11.482	83.064	4.592 2

either 60 or 100 W, and the gas pressure in the chamber was in the 10^{-4} Torr range. Materials were exposed to atomic oxygen along with other charged and uncharged species in the plasma. The flux of atomic oxygen was of the order of 10^{21}–10^{23} atoms/cm^2 s. An *in situ* ellipsometer was used to monitor the entire process. In doing this, the optical constants of the materials were determined as a function of exposure time. This process helped predict the behavior of materials in the space environment. The equivalence between this plasma exposure and the erosion due to the LEO environment was determined by measuring the Kapton weight loss.[3,23,24] According to the Kapton weight loss results, our AO plasma is about 1000 times stronger than the real LEO environment.

3. SE technique and modeling

Spectroscopic ellipsometry is an nondestructive method used to determine film thicknesses and optical constants. The change in polarization state of a reflected light beam with respect to that of the incident light beam is measured over a wide range of wavelengths and at one or more angles of incidence [variable angle spectroscopic ellipsometry (VASE)]. The sample complex reflection coefficients for polarized light beams (parallel to and perpendicular to the plane of incidence), are given by the Fresnel coefficients R_p and R_s, respectively. Ellipsometric parameters Ψ and Δ are related to these coefficients by[25]

$$\rho \equiv \tan(\Psi)e^{i\Delta} = R_p/R_s . \tag{1}$$

With initial estimates for the unknown layer thickness and/or optical constants, a set of Ψ and Δ values are calculated for the known wavelengths and angles of incidence. The weighted mean-square difference between calculated and measured values is calculated, and then minimized using the Levenberg–Marquardt algorithm by varying the model parameters.[26] The thickness and optical constants are then obtained as a result of regression fits. However, the correlation between the optical constants and the thickness is sometimes too large for the accurate determination of both values. In this study, two analytical methods were employed to eliminate this correlation problem.

(a)   *Multisample analysis.* In this analysis, data from multiple samples are fitted simultaneously to different models in which the fitting optical constants are coupled together, assuming that they are the same for all samples. Since film thicknesses are also fitting parameters but are different from sample to sample, the correlation between the two parameters is eliminated.[27]
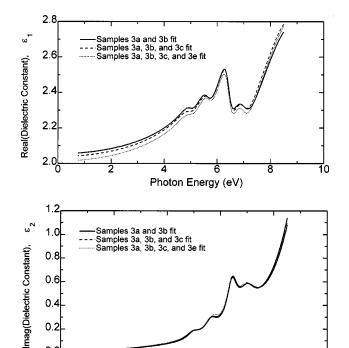
FIG. 3. Compariosn of optical constants obtained from two-, three-, and four-sample multisample analysis.

(b)   *Parametric model:* Instead of fitting the optical constants at each wavelength over the entire spectral range, parametric models such as the Cauchy or Lorentz oscillator model can be applied to reduce the number of variables, and thus reduce the correlation between the optical constants and thicknesses. For nonabsorbing dielectric films, a four-variable Cauchy model can be used very successfully to eliminate correlation problems.

In this study, both multisample analysis and parametric model fits were utilized to determine layer thicknesses and optical constants.
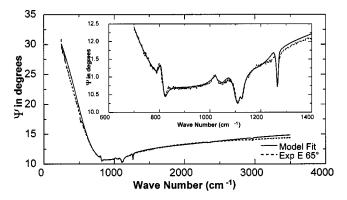

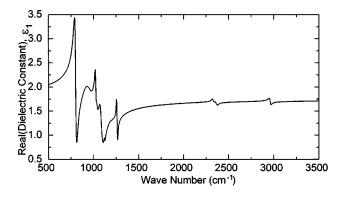FIG. 4. Infrared Se experimental data obtained from sample 3B and the model fit.

B. CV-1144-O optical constants before AO radiation

1. VUV–UV–VIS–NIR

Measurements were performed over a wide spectral range (0.73–6.3 eV) using a standard UV–VIS–NIR, monochrometer-based rotating analyzer ellipsometer on all samples before AO radiation. In addition, vacuum UV (4–8.5 eV) ellipsometric data were taken, using a commercial ellipsometer covering this newly available spectral range. SE data in the VUV–UV–VIS–NIR range are shown in Fig. 2. The CV-1144-O layer thicknesses and optical constants were determined using multisample analysis over the range of 0.73–3 eV, where the silicone film is a pure dielectric (no absorption), and thus the Cauchy model fits quite well. Next, multisample analysis, using a Lorentz oscillator (LO) model, was successfully performed to fit the optical constants over the entire spectral range, as shown in Fig. 2. Multiple absorption peaks were found in the range from 4.8 to 8 eV, and VUV ellipsometry was used to determine the optical constants. A summation of five Lorentzian oscillators was used to fit for the optical constants, with one peak at around 9.2 eV as the background shift. The oscillator constants of the five oscillators are shown in Table II (see, also Table III). Comparisons of optical constants obtained from two-, three-, and four-sample multisample analysis are shown in Fig. 3.

TABLE IV. Peak identification.

Oscillators	Before AO				After AO			
	E_n (cm^{-1})	A_m (eV^2)	B_r (eV)	Characteristic peaks	E_n (cm^{-1})	A_m (eV^2)	B_r (eV)	Strength change
1	802	0.000 771	0.002 97	Si–CH$_3$	804	0.000 376	0.002 21	Decrease
2	858	0.000 347	0.018 9	Unidentified				
3	960	0.435	0.011 9	Unidentified				
4	1024	0.464	0.013 9	Si–O–Si	1022	0.500	0.001 97	Increase
5	1037	0.000 462	0.004 83	Si–O–Si (?)	1037	0.002 03	0.009 23	Increase
6	1087	0.000 953	0.006 38	Si–O–Si	1081	0.001 39	0.007 89	Increase
7	1123	0.105	0.0011	Si–C$_6$H$_5$	1125	0.248	0.010 2	Increase (?)
8	1204	0.114	0.011	Unidentified	1205	0.613	0.009 76	Increase
9	1261	0.703	0.013 6	Si–CH$_3$	1265	0.134	0.001 73	Decrease
10	2330	0.071	0.002 5	Unidentified				
11	2360	0.083	0.003 8	Unidentified				
12	2960	0.000 12	0.002 5	CH$_3$	2960	0.000 062	0.005 49	Decrease

FIG. 5. CV-1144-O optical constants in the IR range.

FIG. 6. SE mapping results from sample 2T before AO radiation.

nant vibrations of specific chemical structures in the CV-1144-O molecule.[28] Optical constants in the IR range are shown in Fig. 5.

3. SE mapping and uniformity study

Before AO exposure, SE mapping experiments were performed on the CV-1144-O silicone samples to inspect the film uniformity. A variable-angle spectroscopic ellipsometry with a sample mapping stage was used for this application. The data were taken at 2.48 eV, and an angle of incidence of 75°. The SE mapping results from sample 2T before AO radiation are shown in Fig. 6. Also shown is the thickness variation over the mapped area. Except for one particular point, the film is very uniform, and the thickness differences are within ± 0.335 nm ($\pm 0.7\%$) over the entire area.

C. AO exposure and *in situ* SE

In this experiment, an ECR oxygen plasma was used to generate atomic oxygen along with many other energetically excited species. The equivalence between this chamber and the LEO environment was evaluated by measuring Kapton weight loss and comparing with data from space. According to these results, the AO radiation strength used was about 1000 times larger than that in LEO, as shown in Table V. For example, weight loss from 1 h in our ECR system corresponds to about 1000 h in space.

CV-1144-O silicone samples were then exposed to the AO plasma under a variety of different conditions. Varied were the exposure time, power, and the oxygen flow rate, as shown in Tables V and VI. The entire erosion process was monitored by *in situ* spectroscopic ellipsometry, and the experimental data from sample 2T are shown in Fig. 7.

Since the optical constants of CV-1144-O change continuously during AO exposure, the established growth-rate (erosion-rate, in this case) fitting method with fixed optical constants is not applicable.[29] However, the fact that the silicone film remains a pure dielectric in this *in situ* SE range (1.62–4.44 eV) justifies using a Cauchy model to determine

Despite slight differences, the optical constants are consistent, which demonstrates the credibility of using multisample analysis.

2. IR

The IR VASE utilizes a rotating polarizer, rotating compensator configuration. The infrared spectra range used was from 8000 to 200 cm^{-1} with a resolution of 2 cm^{-1}. For silicon substrates, in addition to the SE data, transmission data were also taken on undoped substrates, which provided us with more-detailed information. Due to numerous absorption peaks from the thick silicon substrate, the data were so complicated that analysis was almost impossible. Therefore, three other substrates (optically thick films of Au, Pt, and Ir) were developed to eliminate possible information (related to Si) coming from the substrate.

The infrared SE experimental data and the model fit are shown in Fig. 4. Using the determined thicknesses from the Cauchy model, multisample fits described in Sec. III B 1, the optical constants in the IR range were determined using Lorentzian and Gaussian oscillators. Excellent fits were obtained, as shown in Fig. 4. A total of 12 oscillators were used, as shown in Table IV. Some of theme were identified by their oscillator center energies, which correspond to reso-
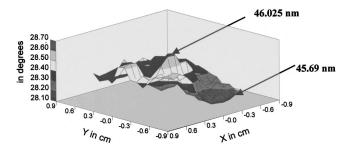
TABLE V. Comparison between the AO chamber in the study and space environment exposure.

Exposure condition	100 W, 2 sccm		60 W, 2 sccm		100 W, 1 sccm		60 W, 1 sccm	
Exposure time	1 hr	2 hr	1 hr	2 hr	1 hr	2 hr	1 hr	2 hr
Time in LEO	1.78 yr	4.04 yr	0.8 yr	1.59 yr	0.28 yr	0.74 yr	0.17 yr	0.36 yr

TABLE VI. Fluences under different exposure conditions. Note: Fluence=change in mass/(density×area ×erosion rate) where the density for Kapton is 1.42 g/cm^3; erosion rate for Kapton is 3.0×10^{-24} cm^3/atom.

Exposure condition	1 hr	2 hr
100 W, 2 sccm	7.40×10^{22} atoms/cm^2	1.68×10^{23} atoms/cm^2
60 W, 2 sccm	3.33×10^{22}	6.62×10^{22}
100 W, 1 sccm	1.16×10^{22}	3.09×10^{22}
60 W, 1 sccm	7.08×10^{21}	1.52×10^{22}

both film thickness and optical constants at every stage of the AO exposure. Excellent Cauchy fits were obtained, and changes in the optical constants and layer thickness as a function of erosion time were determined, as shown in Fig. 8. Notice in Fig. 8(a) that the refractive index of the silicone film increases during AO exposure, indicating that the film densified. The corresponding LEO time is labeled in Fig. 8(b). It is seen that the film thickness in this case decreased (by 14 nm) to about 2/3 of its original value in about two months equivalent LEO time.

D. CV-1144-O optical constants after AO radiation

1. VUV–UV–VIS–NIR

After AO exposure, the same SE measurements were performed on all CV-1144-O samples in the VUV–UV–VIS–NIR spectral range as prior to exposure, and Lorentz oscillator fits for the optical constants were also successful. A comparison of optical constants (before and after AO radiation) is shown in Fig. 9. As a result of AO radiation, both the number and amplitude of the oscillators decreased in the VUV and UV range, indicating less absorption in this range
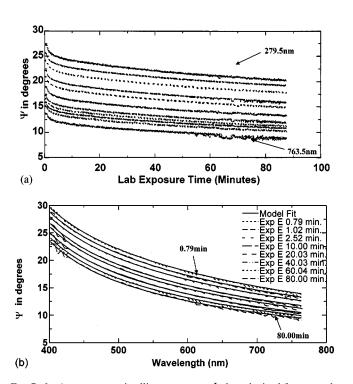
after exposure to the plasma. Instead of having five oscillators in the Lorentzian oscillator model, the postexposure model used only three oscillators. The oscillator constants of these three oscillators are shown in Table III. Notice that the two peaks at 4.2 and 6.4 eV were present both before and after AO exposure, despite the very slight difference in position, which could be due to oscillator fit. After exposure, both these two peaks were broadened, as could also be seen from Tables II and III.

2. IR

IR SE data provided us with detailed information about surface chemical changes. By comparing data before and after AO exposure, some general ideas about what happened chemically during the AO radiation process were determined. A comparison of Lorentz oscillator fit optical constants (before and after AO radiation) is shown in Fig. 10, and the corresponding oscillator parameters are shown in Table IV. As shown in Table IV, after AO radiation, a total
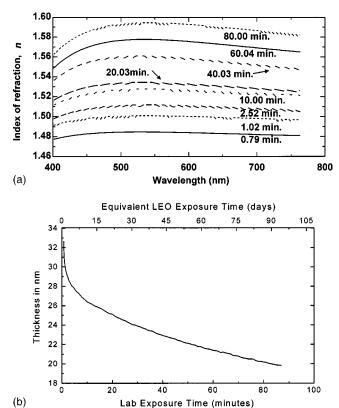
FIG. 7. *In situ* spectroscopic ellipsometry raw Ψ data obtained from sample 2T, vs (a) exposure time for wavelengths from 279.5 to 763.5 nm and (b) wavelength, for exposure time from 0.79 to 80 min.

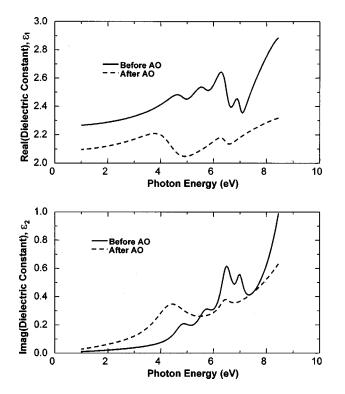FIG. 8. Changes of the optical constants and layer thickness as functions of exposure time (sample 2T). (a) *n*. (b) Thickness.

FIG. 9. Comparison of optical constants before and after AO radiation in the VUV–UV–VIS–NIR spectral range (sample 3B, see Table I).

FIG. 10. Comparison of optical constants before and after AO radiation in the IR (sample 3B, see Table I).

of 9 instead of 12 oscillators were present, which corresponds to fewer characteristic resonant chemical structures after exposure. The double-peaked absorption band near 1000 cm^{-1} was identified as the Si–O stretching band, which is consistent with previous results on the etching of polydimethyl siloxane films in a rf oxygen plasma,[30] and peaks at around 800 and 1200 cm^{-1} were also identified as a Si–O stretching band. Polydimethyl siloxane is quite similar to the CV-1144-O silicone but has a simpler chemical structure in that it lacks the 4.8% benzene ring structure contained in CV-1144-O. As expected, reasonably similar IR spectra were obtained from CV-1144-O silicone samples, with some Si–C_6H_5-realted peaks present ($\sim 1100 \text{ cm}^{-1}$). After AO exposure, the intensity of all CH_3-related peaks decreased, while SiO_x-related peaks increased as a result of AO radiation. This is not unexpected when recalling the chemical structure of the CV-1144-O polymer. When exposed to AO, CV-1144-O is chemically converted into (more AO resistant) SiO_x,[4,5] which is chemically inert toward atomic oxygen, and the pendant groups, mainly CH_3, were converted into volatile CO_2 and H_2O.[22] The significant decrease of the CV-1144-O layer thickness is due to AO-dissociating carbon and hydrogen bonds and forming volatiles (CO, CO_2, H_2, and H_2O).[5,31]

Recalling the VUV results, it is very interesting to see that as the CH_3-realted vibrations in the IR range disappear, the absorbing features in the UV range decrease as well. We conclude that CH_3-based structures are the major structures affected by the AO radiation, and thus may account for breakdown of the CV-1144-O silicone structure.

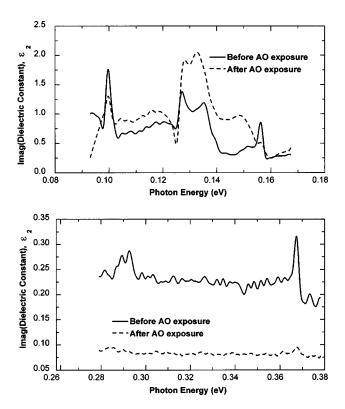Despite all this information, the specific chemical changes

during AO radiation are not well known yet, including the mechanism of how CV-1144-O thin films react with AO, what the erosion products are, and how the volatile materials evolve from the film. We will focus on these questions in the future. For now, the main purpose of this study was to obtain optical constants over the entire spectral range, before and after AO radiation; study chemical conversion and layer thickness changes; and monitor the AO erosion process using *in situ* SE to obtain erosion rates.

III. CONCLUSION

Spectroscopic ellipsometry proved to be of great use in determining optical constants and layer thicknesses of CV-1144-O, as well as studying chemical changes with AO exposure. In addition to UV–VIS–NIR and IR data, vacuum UV ellipsometric data were also taken for the first time, to determine optical constants at short wavelengths. Lorentzian and Gaussian oscillators were used successfully to fit for the optical constants, and the major resonant absorption peaks in the IR region were identified. The comparison between prior- and post-AO-radiation spectra indicated a significant decrease in CH_3-associated peaks and an increase in SiO_x-associated peaks.

In situ SE was used to monitor the erosion process under AO plasma radiation, so that we could see the changes in optical constants and erosion rates with exposure time. Results showed that the erosion rate at the beginning of the process was substantially faster than that at later times. Approximately 14 nm of material (one third of the total silicone

thickness) was eroded away within 1 h in the ECR chamber, corresponding to about two months in low earth orbit. In addition, the refractive index of CV-1144-O in the visible range increased during the process, indicating that the film densified during the exposure.

ACKNOWLEDGMENT

[1]S. L. Koontz, K. Albyn, and L. J. Leger, J. Spacecr. Rockets **28**, 315 (1991).

[2]S. Packirisamy, D. Schwam, and M. H. Litt, J. Mater. Sci. **30**, 308 (1995).

[3]B. A. Banks, K. K. de Groh, E. Baney-Barton, E. A. Sechkar, P. K. Hunt, A. Willoughby, M. Bemer, S. Hope, J. Koo, C. Kaminski, and E. Yougstrom, NASA Tech. Memo. 209180, 1999.

[4]J. A. Dever, NASA Tech. Memo. 103711, 1991.

[5]B. A. Banks, K. K. de Groh, S. K. Rutledge, and F. J. Difilippo NASA Tech. Memo. 107204, 1996.

[6]D. G. Zimcik and C. R. Maag, J. Spacecr. Rockets **25**, 162 (1988).

[7]M. R. Reddy, J. Mater. Sci. **30**, 281 (1995).

[8]S. L. Koontz, L. J. Leger, and J. T. Visentine, J. Spacecr. Rockets **32**, 483 (1995).

[9]J. A. Dever, E. J. Bruckner, D. A. Scheiman, and C. R. Stidham, NASA Tech. Memo. 106592, 1994.

[10]D. G. Zimcik, M. R. Wertheimer, K. B. Balmain, and R. C. Tennyson, J. Spacecr. Rockets **28**, 652 (1991).

[11]*Materials Degradation in Low Earth Orbit (LEO)*, edited by V. Srinivasan and B. A. Banks (The Minerals, Metals and Materials Society, Warrendals, PA, 1990).

[12]G. Czeremuszkin, M. R. Wertheimer, J. Cerny, J. E. Klemberg-Sapieha, and L. Martinu, in *Proceedings of ICPMSE-3, Third International Space Conference,* edited by J. I. Kleiman and R. C. Tennyson (Kluwer Academic, Dordrecht, The Netherlands, 1999).

[13]P. Halevi, *Photonic Probes of Surfaces* (North-Holland, Amsterdam, 1995).

[14]V. F. Kokorina, *Glasses for Infrared Optics* (CRC, Boca Raton, FL, 1996).

[15]J. W. Connell, J. V. Crivello, and D. Bi, J. Appl. Polym. Sci. **57**, 1251 (1995).

[16]J. W. Gilman, D. S. Schlitzer, and J. D. Lichtenhan, J. Appl. Polym. Sci. **60**, 591 (1996).

[17]J. M. Zeigler and F. W. G. Fearon, *Silicon-Based Polymer Science: A Comprehensive Resource* (American Chemistry Society, Washington, DC, 1990).

[18]B. A. Banks, S. K. Rutledge, P. E. Paulsen, and T. J. Steuber, NASA Tech. Memo. 101971, 1989.

[19]J. T. Wolan and G. B. Hoflund, J. Vac. Sci. Technol. A **17**, 662 (1999).

[20]M. J. Meshishnek, W. K. Stuckey, J. S. Evangelsides, L. A. Feldman, R. V. Peterson, G. S. Arnold, and D. R. Peplinsky, NASA Tech. Memo. 100459, **II**, Sec. 5-1 to 5-33, 1988.

[21]R. C. Tennyson, Can. J. Phys. **69**, 1190 (1991).

[22]C. L. Bungay, T. E. Tiwald, D. W. Thompson, M. J. DeVries, J. A. Woollam, and J. F. Elman, Thin Solid Films **313-314**, 714 (1998).

[23]B. A. Banks, S. K. Rutledge, K. K. de Groh, C. R. Stidham, L. Debauer, and C. M. LaMoreaux, NASA Tech. Memo. 106855, 1995.

[24]A. Snyder, NASA Tech. Memo. 209178, 1999.

[25]R. M. A. Azzam and N. M. Bashara, *Ellipsometry and Polarized Light* (North-Holland, New York, 1977).

[26]G .E. Jellison, Jr., Appl. Opt. **30**, 3354 (1991).

[27]C. M. Herzinger, B. Johs, W. A. McGahan, J. A. Woollam, and W. Paulson, J. Appl. Phys. **83**, 3323 (1998).

[28]*Handbook of Infrared and Raman Spectra of Inorganic Compounds and Organic Salts*, edited by R. A. Nyquist and R. O. Kagel (Academic, San Diego, CA, 1997).

[29]X. Gao, S. Heckens, and J. A. Woollam, J. Vac. Sci. Technol. A **16**, 429 (1998).

[30]N. J. Chou, C. H. Tang, J. Paraszczak, and E. Babich, Appl. Phys. Lett. **46**, 31 (1985).

[31]L. J. Leger and J. T. Visentine, J. Spacecr. Rockets **23**, 505 (1986).